THE JOURNAL OF BIOLOGICAL CHEMISTRY VOL. 288, NO. 32, pp. 23064–23074, August 9, 2013

The UDP-glucose Dehydrogenase of *Escherichia coli* K-12 Displays Substrate Inhibition by NAD That Is Relieved by Nucleotide Triphosphates*

Received for publication, May 22, 2013, and in revised form, June 19, 2013 Published, JBC Papers in Press, June 21, 2013, DOI 10.1074/jbc.M113.486613

Iain L. Mainprize, Jordan D. Bean, Catrien Bouwman, Matthew S. Kimber, and Chris Whitfield[1]

From the Department of Molecular and Cellular Biology, University of Guelph, Guelph, Ontario N1G 2W1, Canada

Background: UDP-glucose dehydrogenase (Ugd) from *E. coli* K-12 is reported to be activated by tyrosine phosphorylation.
Results: Ugd displayed NAD substrate inhibition that could be relieved by the addition of a nucleotide triphosphate in the absence of kinase.
Conclusion: Nucleotide triphosphates are allosteric activators of Ugd.
Significance: Tyrosine phosphorylation is not required for Ugd activation.

UDP-glucose dehydrogenase (Ugd) generates UDP-glucuronic acid, an important precursor for the production of many hexuronic acid-containing bacterial surface glycostructures. In *Escherichia coli* K-12, Ugd is important for biosynthesis of the environmentally regulated exopolysaccharide known as colanic acid, whereas in other *E. coli* isolates, the same enzyme is required for production of the constitutive group 1 capsular polysaccharides, which act as virulence determinants. Recent studies have implicated tyrosine phosphorylation in the activation of Ugd from *E. coli* K-12, although it is not known if this is a feature shared by bacterial Ugd proteins. The activities of Ugd from *E. coli* K-12 and from the group 1 capsule prototype (serotype K30) were compared. Surprisingly, for both enzymes, site-directed Tyr → Phe mutants affecting the previously proposed phosphorylation site retained similar kinetic properties to the wild-type protein. Purified Ugd from *E. coli* K-12 had significant levels of NAD substrate inhibition, which could be alleviated by the addition of ATP and several other nucleotide triphosphates. Mutations in a previously identified UDP-glucuronic acid allosteric binding site decreased the binding affinity of the nucleotide triphosphate. Ugd from *E. coli* serotype K30 was not inhibited by NAD, but its activity still increased in the presence of ATP.

UDP-glucuronic acid (UDPGA)[2] is an essential substrate for biosynthesis of several important glycoconjugates. In multicellular eukaryotes, UDPGA is a precursor for the synthesis of proteoglycans and glycosaminoglycans (1). In both Gram-positive and Gram-negative bacteria, UDPGA is a substrate in the production of many bacterial surface glycostructures, including capsular polysaccharides (CPSs), secreted exopolysaccharides, lipopolysaccharides (LPSs), and teichuronic acids. Bacterial surface glycoconjugates are often critical virulence factors, so UDPGA synthesis can have a direct effect on bacterial pathogenicity. For instance, UDPGA is essential for the formation of hexuronic acid-containing CPSs that often protect bacteria from phagocytosis (2, 3). It is also required to synthesize 4-aminoarabinose, which is used to modify the lipid A core of some bacterial LPSs, resulting in resistance to polycationic compounds (4). UDP-glucose dehydrogenase (Ugd) is the enzyme responsible for generating the activated nucleotide sugar from UDP-glucose (UDPG), coincident with the reduction of NAD (5). The enzyme is conserved in prokaryotes and eukaryotes (6). Human Ugd forms a hexameric ternary complex (7) that can be regulated by feedback inhibition of a downstream product, UDP-xylose (8). Bacterial Ugd enzymes exist as dimers (9–11). In recent years, the structures of a few bacterial homologs of Ugd have been determined, and the kinetics and modes of regulation have been investigated. In the context of this study, the structure of *Klebsiella pneumoniae* Ugd (Fig. 1*B*), in complex with substrate and cofactor (11), is particularly important. One form of regulation that has come under scrutiny is activation of bacterial Ugd by tyrosine phosphorylation by bacterial tyrosine kinases (BY-kinase) (12).

Bacterial BY-kinases are frequently found as part of the machinery catalyzing the assembly of a large and diverse subset of extracellular polysaccharides (12–14). They are sometimes found as a domain of a subfamily of polysaccharide co-polymerase proteins associated with capsular and exopolysaccharide production systems. These proteins possess a transmembrane modulator domain and a cytoplasmic catalytic domain with tyrosine kinase activity. In *Escherichia coli*, these two domains are consolidated into a single polypeptide (designated Wzc) (15, 16), but the domains are encoded as separate polypeptides in Gram-positive bacteria (12). In *E. coli* capsule systems, the polysaccharide co-polymerase protein transmembrane domain interacts with an octameric outer membrane channel (Wza) to form part of the export system for completed polysaccharides (17, 18). The purified BY-kinase domains from *Bacillus subtilis* (YwqC, the transmembrane modulator, and

* This work was supported by Canadian Institutes of Health Research Operating Grant FRN-9623 (to C. W.) and National Science and Engineering Research Council of Canada Grant 327280 (to M. S. K.).

[1] Recipient of a Canada Research Chair. To whom correspondence should be addressed: Dept. of Molecular and Cellular Biology, University of Guelph, 50 Stone Rd. East, Guelph, Ontario, N1G 2W1, Canada. Tel.: 519-824-4120 (Ext. 53361); E-mail: cwhitfie@uoguelph.ca.

[2] The abbreviations used are: UDPGA, UDP-glucuronic acid; AMPPNP, 5′-(β,γ-imido)triphosphate; CPS, capsular polysaccharide; PDB, Protein Data Bank; UDPG, UDP-glucose; Ugd, UDP-glucose dehydrogenase; BY-kinase, bacterial tyrosine kinase.

PtkA, the kinase) have been reported to phosphorylate the *B. subtilis* Ugd homolog (Ugd_{Bs}) *in vitro*, resulting in an ~2-fold increase in Ugd_{Bs} activity (19). This result led to the proposal that phosphorylated Ugd_{Bs} is the active form of the enzyme. Similar experiments implicated phosphorylation in the regulation of Ugd activity in *E. coli* K-12 (20).

E. coli isolates may contain two BY-kinases. The Wzc protein is part of the assembly pathway for serotype-specific group 1 capsular polysaccharides, or colanic acid, which is produced by isolates lacking group 1 capsules, including *E. coli* K-12 (21). Colanic acid is an environmentally regulated exopolysaccharide, which is activated by the Rcs regulon (22). Group 1 CPSs are constitutively expressed virulence determinants (23) and are encoded by gene clusters that occupy the same chromosomal location as the colanic acid genes (24). Consequently, possession of colanic acid and group 1 capsule assembly machinery appears to be mutually exclusive. The second BY-kinase, Etk, is encoded at an unlinked locus that is not expressed in all isolates (25) but can contribute to the formation of group 1 CPSs (26). Etk and Wzc are structural homologs (27, 28).

The *ugd* gene is located near the colanic acid/group 1 CPS locus. It has been proposed that Ugd from *E. coli* K-12 ($Ugd_{K\text{-}12}$) can be phosphorylated by either Etk or Wzc (29); phosphorylation by Wzc is correlated with production of colanic acid, whereas phosphorylation by Etk promotes the synthesis of 4-aminoarabinose for lipid A modification. This study was initially undertaken to investigate the possible role of Ugd phosphorylation in the production of a constitutively expressed CPS. *In vitro* characterization indicated a significant difference in the activities of the two Ugd homologs; $Ugd_{K\text{-}12}$ displays significant levels of NAD substrate inhibition, although Ugd from *E. coli* serotype K30 (Ugd_{K30}) does not. We could not establish an obvious role for phosphorylation in modulating activity of Ugd, but kinetic analyses revealed a novel mechanism of activation that is NTP-dependent.

EXPERIMENTAL PROCEDURES

Bacterial Strains, Plasmids, and Growth Conditions—The bacterial strains and plasmids used in this study are listed in Table 1. All bacterial cultures were grown at 37 °C in lysogeny broth media (30) containing arabinose (0.02–0.1%), galactose (0.04%), and antibiotics (kanamycin at 50 μg/ml and/or ampicillin at 100 μg/ml and/or chloramphenicol at 34 μg/ml), as required. For plasmid nomenclature, ApR, KmR, CmR, and GmR represent ampicillin resistance, kanamycin resistance, chloramphenicol resistance, and gentamicin resistance, respectively.

Construction of Chromosomal Deletion Mutants in E. coli W3110 and E. coli E69—E. coli CWG876, a derivative of *E. coli* K-12 strain W3110 containing Δ*wzc* Δ*etk* and *ugd*::*kan* mutations, was constructed using the λRed recombinase system (31) in a multistep process. Each gene was first completely replaced with a kanamycin resistance cassette, and then the cassette was excised using the pCP20 helper plasmid (32), before subsequent genes were deleted. The kanamycin resistance cassette was not removed from the chromosome in the final mutant strain as the marker had no bearing on subsequent experiments. Gene deletions were confirmed by PCR.

TABLE 1
Bacterial strains and plasmids

	Description	Ref.
Strains		
E.coli DH5α	ϕ80d *deoR lacZΔM15 endA1 recA1 hsdR17* ($r_K^- m_K^-$) *supE44 thi-1 gyrA96 relA1* Δ (*lacZYA-argF*)*U169* F^-	
E. coli E69	Prototroph, serotype O9a:K30:H12	I. Orskov
E.coli W3110	F^- λ^- IN (*rrnD-rrnE*)1 *rph-1*	
CWG285	E69 wzc_{K30}::*aacC1*; wza_{22min}::*aadA* (polar on *etp* and *etk*); Gm^R, Sp^R	26
CWG875	E69 Δ*galE ugd*::*aaC1*; Gm^R	This study
CWG876	W3110 Δ*wzc* Δ*etk ugd*::*kan*; Km^R	This study
Plasmids		
pBAD18, pBAD24, pBAD33	Arabinose-inducible expression vectors; Km^R or Ap^R or Cm^R	56
pWQ173	Allelic exchange suicide vector with *pheS* gene; Cm^R	23
pWQ500	pHC79 derivative containing *E. coli* E69 chromosomal region surrounding $rcsA_{K30}$; Ap^R	57
pWQ629	pUC19 derivative containing *E. coli* E69 chromosomal region surrounding ugd_{K30}	37, 58
pWQ728	pWQ173 derivative containing ugd_{K30} interrupted with gentamicin resistance cassette at SacI site; Gm^R, Cm^R	This study
pWQ729	pBAD24 derivative expressing His_6-$Ugd_{K\text{-}12}$; Ap^R	This study
pWQ730	pBAD24 derivative expressing His_6-Ugd_{K30}; Ap^R	This study
pWQ731	pWQ729 derivative containing Y71F mutation; Ap^R	This study
pWQ732	pWQ730 derivative containing Y71F mutation; Ap^R	This study
pWQ733	pWQ729 derivative containing K323A mutation; Ap^R	This study
pWQ734	pWQ729 derivative containing R324A mutation; Ap^R	This study
pWQ735	pWQ729 derivative containing KR → AA mutations at residues 323–324; Ap^R	This study
pWQ736	pBAD18 derivative expressing His_6-$Wzc_{K\text{-}12}$ residues 447–704; Ap^R	This study
pWQ737	pBAD18 derivative expressing His_6-Wzc_{K30} residues 447–704; Ap^R	This study
pWQ738	pBAD33 derivative expressing His_6-$Ugd_{K\text{-}12}$; Cm^R	This study
pWQ739	pBAD33 derivative expressing His_6-Ugd_{K30}; Cm^R	This study

Mutation of *ugd* in *E. coli* serotype K30 affected growth of the organism, presumably due to the accumulation of incomplete capsular polysaccharide repeat units. This led to the accumulation of second-site suppressor mutants, as seen in comparable biosynthetic systems (33, 34). To make CWG875, an *E. coli* serotype K30 (strain E69) derivative with a *ugd* deletion, the *galE* gene was first deleted to generate a strain where K30 capsular polysaccharide production was conditional. GalE (UDP-galactose-4-epimerase) is required for synthesis of the precursor for the galactose residues for the K30 repeat units, one of which is the first sugar of the repeat unit (35). The deletion of *galE* stops the synthesis of the CPS at the initial step of building the repeat unit on a carrier lipid thereby preventing the production of any synthesis intermediates whose accumulation could affect cell fitness and/or survival. To provide permissive conditions for K30 antigen production, the absence of GalE is overcome by addition of galactose to the growth medium (36). The *galE* gene was replaced with the kanamycin resistance cassette using the λRed recombinase system, and the cassette was excised, as above. The ugd_{K30} gene was disrupted with a gen-

tamicin resistance cassette, using a suicide delivery vector (pWQ173), using a method reported elsewhere (23). Under nonpermissive conditions for CPS synthesis, the *ugd* mutation was tolerated. This provided a background where function of plasmid-encoded Ugd proteins could be tested *in vivo* based on their ability to restore CPS production under permissive conditions.

Amplification and Mutagenesis of ugd Gene—The $ugd_{K\text{-}12}$ gene was PCR-amplified from *E. coli* DH5α genomic DNA with primers JB2 and JB6 that incorporate the coding sequence for an N-terminal hexahistidine (His_6) tag. The resulting PCR product was cloned into pBAD24 to generate pWQ729. The ugd_{K30} gene was amplified from pWQ629 (37), incorporating the His_6 tag and cloned into pBAD24, generating pWQ730. The QuikChange mutagenesis protocol (Stratagene/Agilent Technologies) was used to make site-directed mutants of $Ugd_{K\text{-}12}$ and Ugd_{K30}. Mutagenic primer pairs (primer sequences available upon request) were synthesized by Sigma, and DNA was amplified using Pfu Ultra DNA polymerase (Stratagene/Agilent Technologies). Mutations were confirmed by DNA sequencing at the Advanced Analysis Centre (University of Guelph).

DNA fragments encoding His_6-tagged $Ugd_{K\text{-}12}$ and Ugd_{K30} were excised from pWQ729 and pWQ730, respectively, by digestion with BamHI and HindIII and then cloned into pBAD33 producing pWQ738 and pWQ739, respectively. These pBAD33-based plasmids were compatible with the *rcsA*-containing pWQ500 for co-transformations of W3110.

Ugd Purification—His_6-tagged $Ugd_{K\text{-}12}$ and Ugd_{K30} proteins were expressed and purified primarily from CWG876 (exceptions to this are noted where relevant). Overnight cultures were diluted 1:50 into 1 liter of lysogeny broth media and grown at 37 °C to an $A_{600} = 0.4 - 0.6$, at which time arabinose was added to a final concentration of 0.02%. After 3 more hours of growth at 37 °C, cells were collected by centrifugation at 5,000 × *g* for 10 min at 4 °C. Cell pellets were resuspended in 20 mM sodium phosphate, pH 7.0, containing Complete Mini, EDTA-free protease inhibitor tablets (Roche Diagnostics), RNase (0.375 mg/ml, Roche Diagnostics), and DNase (0.375 mg/ml, Roche Diagnostics). The cells were then lysed by sonication. After centrifugation (1 h at 100,000 × *g*) to remove cell debris and unbroken cells, the lysate was incubated with nickel-nitrilotriacetic acid resin (Qiagen) for 1 h with mixing at 4 °C. The resin was poured into a column, and the flow-through was collected. Loosely bound proteins were removed with sequential washes of Buffer A (50 mM Tris-HCl, pH 7.5, 300 mM NaCl, 10 mM β-mercaptoethanol, and 10% glycerol) containing increasing concentrations of imidazole (10 and 40 mM). Ugd was then eluted with Buffer A containing 250 mM imidazole. The elution buffer in the protein samples was replaced with Buffer B (50 mM Tris-HCl, pH 7.5, containing 100 mM NaCl, 1 mM EDTA, 1 mM DTT, and 10% glycerol) by passage over a PD-10 desalting column (GE Healthcare). Protein concentration was determined using protein assay (Bio-Rad).

Ugd Activity and Kinetics Analysis—The UDP-glucose dehydrogenase activity of Ugd was measured using a version of a spectrophotometric assay (38), modified to facilitate the use of 96-well plates. The dehydrogenase reaction contained Buffer C (100 mM glycine, pH 9.5, 100 mM NaCl, 0.1 mg/ml acetylated BSA, and 10% glycerol). NAD and UDPG were varied as required (maximal concentrations were 5 mM for both). Reactions were monitored by absorbance at 340 nm in a temperature-controlled BMG FLUOStar OPTIMA plate reader. K_m, K_{si}, and V_{max} values were calculated using the GraphPad Prism4 software program (GraphPad Software, Inc.), by fitting the data to the equation $Y = V_{max} \cdot X \, (K_m + X \cdot (1 + X/K_{si}))$, where Y is the enzyme velocity; X is the substrate concentration; V_{max} is the maximum enzyme velocity; K_m is the Michaelis-Menten constant, and K_{si} is the substrate inhibition constant. K_m and K_{si} values are expressed in the same units as the substrate concentration (X). Reactions were performed in triplicate (unless otherwise noted).

For pretreatment with kinase, nucleotides, and/or cation additives, purified Ugd (1 μg of Ugd per 125 μl reaction) was incubated for 10 min at 37 °C with the appropriate additive in the presence of Buffer B. To measure the dehydrogenase activity, 30 μl of the pretreatment reactions (or an equivalent concentration of Ugd) was combined with reaction mixture in a final volume of 200 μl.

SDS-PAGE and Western Blotting—Proteins were examined by SDS-PAGE using 10% resolving gels. K30 CPS production was monitored by immunoblotting of proteinase K-treated whole-cell lysates (39). SDS-PAGE and immunoblotting with anti-K30 antibodies (40) were performed as described previously (41).

In Vivo Phosphorylation Status of Ugd—Production of colanic acid was induced in wild-type *E. coli* K-12 strain, W3110, with the introduction of plasmid pWQ500, encoding the transcriptional regulator RcsA (57). Overexpression of His_6-tagged Ugd proteins (encoded on plasmids pWQ738 and pWQ739) in cells carrying pWQ500 was also done to improve the detection of a potential tyrosyl-phosphorylated Ugd. Cell lysates were separated by SDS-PAGE, and proteins were visualized by immunoblotting with antibodies specific to phosphotyrosine (PY20, Sigma).

Structural Model of $Ugd_{K\text{-}12}$—The model of $Ugd_{K\text{-}12}$ was generated by SWISS-MODEL using the "automated mode." The template was provided by the structure of the protein from *K. pneumoniae* (Ugd_{Kp}) in complex with NAD and uridine 5′-monophosphate (PDB 3PLR (11)). To obtain a better representation of a molecule of UDPG in the active site, the structure of Ugd_{Kp} in complex with UDPGA (PDB 3PJG) was aligned to the $Ugd_{K\text{-}12}$ model by PyMOL (PyMOL Molecular Graphics System Version 0.99rc6, Schrödinger, LLC), and an oxygen atom on C6 of the glucose moiety of UDPGA molecule was removed.

RESULTS

$Ugd_{K\text{-}12}$ Can Functionally Replace Ugd_{K30} in Biosynthesis of K30 CPS—The Ugd proteins from *E. coli* K-12 and the K30 serotype strain, E69 (hereafter referred to as $Ugd_{K\text{-}12}$ and Ugd_{K30}, respectively), are recently diverged homologs sharing 82% sequence identity and 93% similarity (Fig. 1*A*). Both proteins possess the Tyr-71 residue, which is the proposed site of tyrosine phosphorylation in $Ugd_{K\text{-}12}$ (29). However, there is some sequence diversity in the region of this residue (Fig. 1*A*), giving rise to the possibility that the two proteins may differ in

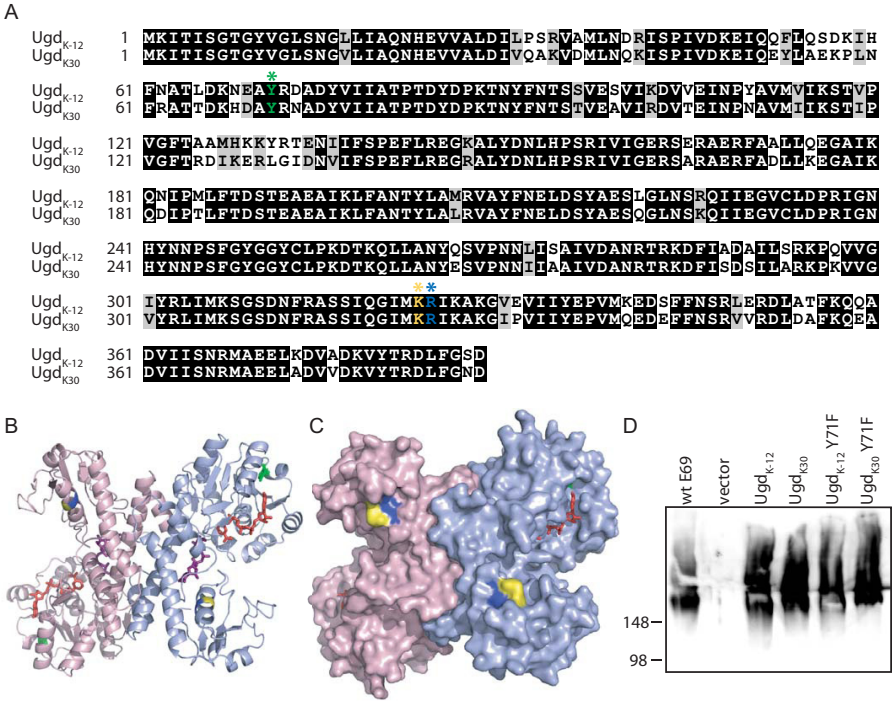

FIGURE 1. **Sequence alignment and complementation of CWG875 by Ugd_{K-12} and Ugd_{K30}.** *A*, amino acid sequences were aligned by Clustal (59). Identical and similar residues are highlighted in *black* and *gray*, respectively (by Boxshade). The proposed site of tyrosine phosphorylation (Tyr-71) is indicated by a *green asterisk*. Lys-323 and Arg-324 are indicated by *yellow* and *blue asterisks*, respectively. *B*, model of Ugd_{K-12} displayed as a dimer (protomers colored *light blue* and *pink*). NAD (*red sticks*), UDPG (*purple sticks*), and tyrosine 71 (*green sticks*) are displayed. Lys-323 and Arg-324 are colored *yellow* and *blue*, respectively. *C*, surface representation of the model of Ugd_{K-12} colored as in *B*. *D*, immunoblotting of proteinase K-treated cell lysates of CWG875 expressing Ugd homologs (and Y71F mutants of each) probed with antibodies specific for the K30 capsular polysaccharide. See Table 1 for plasmid assignments. Plasmid pBAD24 was used for sample labeled *vector*.

either the efficiency or the effects of phosphorylation at this position. Activity of Ugd_{K30} is required for the production of K30 CPS in *E. coli* E69, so CPS production from a *ugd* deletion strain reflects the *in vivo* functioning of plasmid-encoded Ugd proteins. An additional Δ*galE* mutation in this background made CPS production conditional on addition of galactose to the growth medium (see "Experimental Procedures").

Expression of His_6-tagged Ugd_{K-12} restored K30 CPS production in CWG875 (Δ*galE* Δ*ugd*), as shown by immunoblotting cellular extracts with K30-specific antibodies (Fig. 1*D*). Therefore, any regulatory elements required for Ugd_{K-12} are met in the group 1 capsule-producing background. Surprisingly, a Tyr → Phe mutation at the proposed site of phosphorylation, Tyr-71, did not have any detectable effect on the ability of Ugd_{K-12} to function in K30 CPS synthesis. In previous reports, a Ugd_{K-12} Y71F mutant showed very low activity *in vitro* (29). In addition, when examined in an *E. coli* K-12 background where colanic acid expression was activated, the Y71F mutant protein resulted in drastically reduced levels of colanic acid and a corresponding loss of the mucoid colony phenotype. In CWG875, the Tyr-71 residue of Ugd_{K30} was also not essential for K30 CPS production. In the context of a constitutively expressed capsular polysaccharide, the proposed phosphorylation site of Ugd was therefore not required in either of the Ugd homologs.

Ugd Is Active in the Absence of Phosphorylation—These results suggested that either redundant phosphorylation sites exist or that Ugd phosphorylation is not required for K30 capsule production. To rule out the possibility of phosphorylation occurring on a different residue in Ugd, the genes encoding the only two known BY-kinases in *E. coli* K-12 were deleted to generate strain CWG876 (W3110 Δ*wzc* Δ*etk ugd*::*kan*). The dehydrogenase activities of purified Ugd proteins isolated from CWG876 were analyzed at fixed substrate concentrations (Fig. 2*A*). Consistent with the *in vivo* activities of the Y71F mutants, both Ugd homologs expressed in the kinase-deficient background were enzymatically active, although the activity of Ugd_{K-12} was considerably lower than Ugd_{K30}. The activity of Ugd_{K-12} isolated from CWG875 (*i.e.* a BY-kinase-positive strain) was indistinguishable from the same protein prepared from the kinase-deficient background. Furthermore, we could not detect any phosphorylation of Ugd_{K-12} *in vivo* in *E. coli* under conditions where the *wzc* kinase gene was derepressed and colanic acid production was activated by the overexpression of the transcriptional regulator RcsA (data not shown).

Ugd Activity Is Stimulated by Triphosphate Esters—It was previously reported that incubation of Ugd_{K-12} with the kinase domain of Wzc and ATP resulted in a modest increase in Ugd activity (20). We observed similar results (data not shown), but this was inconsistent with the results described above. To investigate this phenomenon in more detail, the contents of the phosphorylation reactions were examined systematically. Surprisingly, an ~6-fold increase in Ugd_{K-12} activity was observed when only ATP was added to the reaction (Fig. 2*A*). A substantial increase in Udg_{K30} activity was also observed when ATP was added, but in this case, the increase was not as large, possibly because Ugd_{K30} has a higher basal activity than Ugd_{K-12}. To rule out the possibility that enzyme activation resulted from

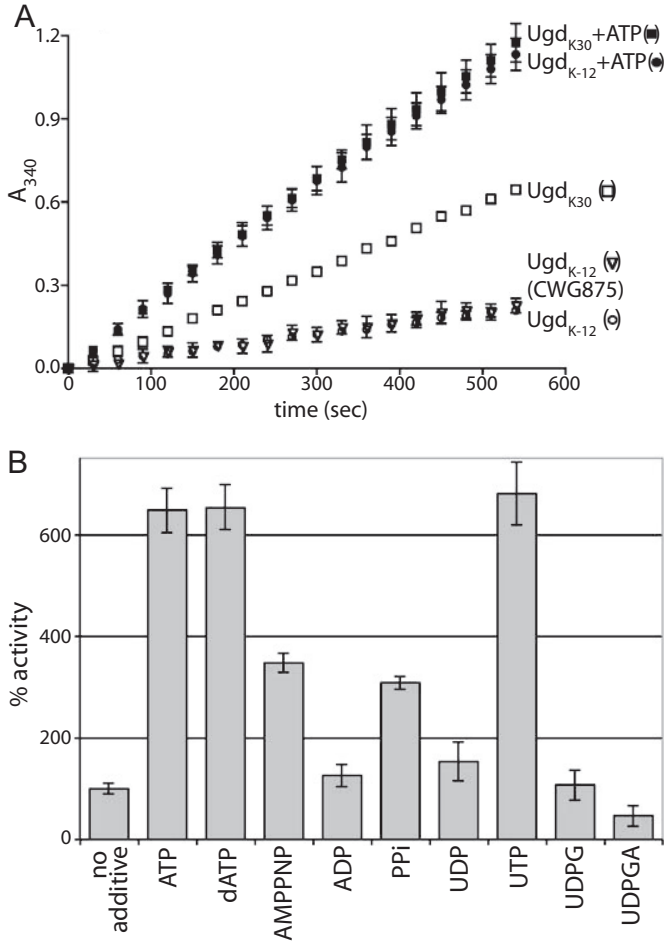

FIGURE 2. **Activation of Ugd dehydrogenase activity.** *A*, activities of Ugd_{K-12} and Ugd_{K30} purified from CWG876 were monitored over 10 min in the presence or absence of 1 mM ATP, at fixed concentrations of 5 mM NAD and 5 mM UDPG. The activity of Ugd_{K-12} purified from CWG875 was included as a control for a BY-kinase-positive strain. *B*, other nucleotides and pyrophosphate were tested for the ability to affect Ugd_{K-12} activity. All were added to a concentration of 1 mM. The slope of a line produced by plotting the A_{340} *versus* time (as in *A*) was calculated and normalized to the "no additive" reaction, which was arbitrarily set to 100%. All reactions were tested in triplicate (except for the Ugd_{K30} reaction, which was done in duplicate), and standard deviations are shown as *error bars*. The NAD and UDPG substrates were fixed at 5 mM for all reactions (except for the reaction with added UDPG).

trace amounts of phosphorylation by the activity of a contaminating kinase, the effect of AMPPNP was examined. This nonhydrolyzable analog of ATP also caused an increase in the activity of Ugd_{K-12}, although to a lower extent than ATP (Fig. 2*B*). Other nucleotides were tested for the ability to activate Ugd_{K-12}; all of the tested nucleotide triphosphates (including dATP) were able to increase the activity of Ugd_{K-12}. In contrast, nucleotide diphosphates and the nucleotide sugar substrate, UDPG, did not affect the activity. Consistent with product inhibition observed with other Ugd homologs (11, 42), UDPGA caused a decrease in Ugd_{K-12} activity. As any tested NTP (or dNTP) was able to cause the activity increase, and NDP was not able to activate, the triphosphate ester moiety appears to be the shared "activating" feature. Highlighting the importance of the phosphate groups, pyrophosphate was able to increase the activity to an intermediate level (on par with AMPPNP).

Kinetic Parameters for Ugd Dehydrogenase Activity—The demonstrable lack of requirement for a kinase in Ugd activation indicated that there is some other underlying mechanism for the NTP-dependent activation of Ugd_{K-12}. To investigate this further, the kinetics of the enzyme were analyzed. At a fixed UDPG concentration, the dehydrogenase activity of Ugd_{K-12} decreased at NAD concentrations above 1 mM (Fig. 3), indicating substrate inhibition. A kinetic model that includes substrate inhibition gave a satisfactory fit for the plot of activity *versus* NAD concentration and resulted in a calculated K_{si} for NAD of

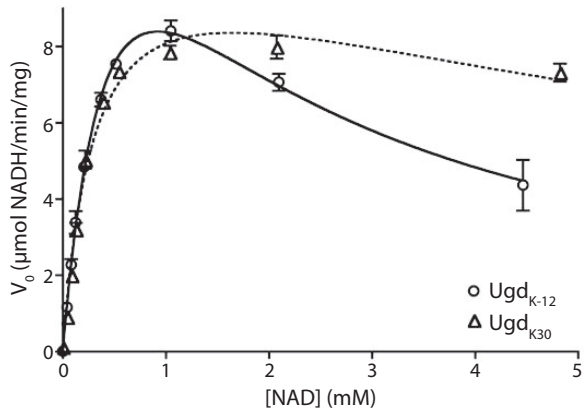

FIGURE 3. **NAD kinetics for Ugd_{K-12} and Ugd_{K30}.** The initial reaction velocities of Ugd_{K-12} and Ugd_{K30} were calculated over a range of NAD concentrations at a fixed UDPG concentration (5 mM). *Lines* representing the best fit of substrate inhibition kinetics were plotted for both homologs. *Error bars* represent the standard deviation of reactions done in triplicate.

TABLE 2

Kinetic parameters for NAD of Ugd_{K-12} and Ugd_{K30} isolated from CWG876

	k_{cat}	K_m	K_{si}
	s^{-1}	mM	mM
Ugd_{K-12}	7.1 ± 0.5	0.62 ± 0.07	1.4 ± 0.2
Ugd_{K30}	4.2 ± 0.2	0.31 ± 0.03	8.7 ± 1.6
Ugd_{K-12} Y71F[a]	7.3 ± 0.9	0.50 ± 0.10	1.4 ± 0.3
Ugd_{K-12} K323A	2.7 ± 0.2	0.43 ± 0.05	2.8 ± 0.4
Ugd_{K-12} + [ATP] (μM)			
25	5.9 ± 0.4	0.45 ± 0.05	2.6 ± 0.3
50	6.2 ± 0.4	0.62 ± 0.06	2.8 ± 0.4
100	5.3 ± 0.2	0.45 ± 0.03	5.4 ± 0.7
250	5.1 ± 0.3	0.45 ± 0.04	13.4 ± 3.7
500	5.0 ± 0.2	0.35 ± 0.03	24.9 ± 7.9
750	5.6 ± 0.3	0.44 ± 0.04	30.9 ± 15.2
1000	5.5 ± 0.2	0.38 ± 0.03	47.4 ± 27.0

[a] Ugd_{K-12} Y71F was tested in duplicate; all others were tested in triplicate.

TABLE 3

Kinetic parameters for NAD of Ugd_{K-12} isolated from wild-type and BY-kinase deletion strains

	k_{cat}	K_m	K_{si}
	s^{-1}	mM	mM
Wild-type E69	5.7 ± 0.4	0.45 ± 0.05	1.3 ± 0.2
CWG285	5.4 ± 0.4	0.35 ± 0.04	1.5 ± 0.2
Wild-type W3110	6.1 ± 0.4	0.45 ± 0.04	1.9 ± 0.2
CWG876	7.1 ± 0.5	0.62 ± 0.07	1.4 ± 0.2

1.4 ± 0.2 mM (Table 2). Conversely, the activity of Ugd_{K30} reached a plateau at high concentrations of NAD, and the resulting plot conformed more closely to classical Michaelis-Menten kinetics. When analyzed with a substrate inhibition model, the Ugd_{K30} K_{si} for NAD was five times higher than that for Ugd_{K-12} (Table 2). In summary, there may be some NAD substrate inhibition for Ugd_{K30}, but it plays a relatively minor role at the concentrations used in these experiments. The other kinetic parameters were relatively similar for the two homologs (see Table 2). Additionally, Ugd_{K-12} purified from wild-type serotype K30 and wild-type W3110 (both of which contain endogenous *etk* and *wzc* genes) showed kinetic parameters virtually identical to Ugd_{K-12} purified from related BY-kinase deletion strains, CWG285 and CWG876 (Table 3).

Consistent with the ability of the Y71F mutant of Ugd_{K-12} to substitute *in vivo* for wild-type protein, the kinetic parameters of this mutant were similar to the wild-type protein (Table 2). However, the purified Ugd_{K-12} Y71F mutant protein was highly prone to aggregation and loss of activity in the absence of glycerol in the reaction buffer (Fig. 4). To overcome any potential problems with aggregation, glycerol was included in the buffers in all of the experiments presented here (unless otherwise noted).

To determine whether the NTP-dependent activation of Ugd_{K-12} influenced the kinetics of the dehydrogenase, the NAD reduction kinetics were analyzed in the presence of increasing ATP (Fig. 5). As the concentration of ATP increased, the substrate inhibition due to NAD diminished, resulting in a corresponding ATP-dependent increase in K_{si} for NAD (Table 2). At higher ATP concentrations, the activity plot for Ugd_{K-12} appeared to follow Michaelis-Menten kinetics. Replacing ATP with AMPPNP or pyrophosphate had a similar effect on the NAD substrate inhibition (data not shown), consistent with the observation that this effect is not specific to ATP.

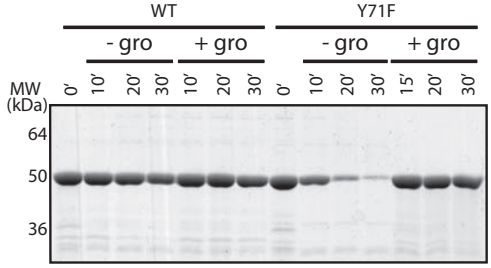

FIGURE 4. **Stability of Ugd_{K-12}.** Wild-type and Y71F mutant Ugd_{K-12} proteins were incubated at 37 °C in the presence/absence of glycerol (*gro*, 10% v/v final concentration) for the times indicated. Samples were subjected to centrifugation at maximum speed (16,100 × *g*) for 5 min in a microcentrifuge. The resulting supernatants were separated by SDS-PAGE and stained with Simply Blue (Invitrogen).

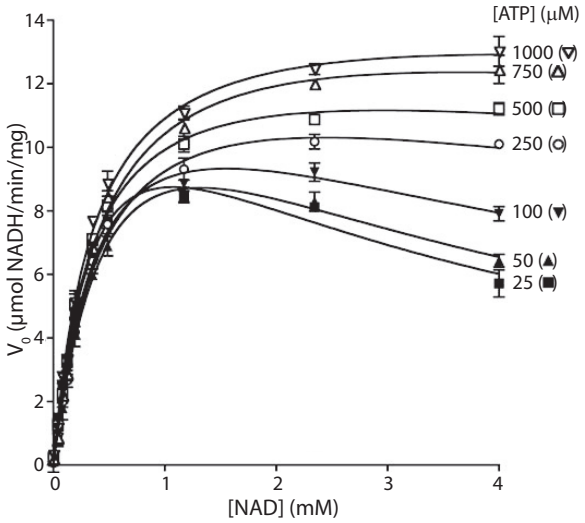

FIGURE 5. **ATP addition removes the NAD substrate inhibition of Ugd_{K-12} in a concentration-dependent manner.** The substrate inhibition kinetics of Ugd_{K-12} were monitored and plotted, as in Fig. 3, with increasing ATP concentrations. There was an outlier at 100 μM NAD for the 750 μM ATP run that was removed.

During assay optimization, it was found that the inclusion of $MgCl_2$ in the reaction buffer could reverse the NTP-dependent activation of Ugd_{K-12}, in a concentration-dependent manner (Fig. 6*A*). This was not specific to Mg^{2+} as a similar effect was found for other divalent cations, including Ca^{2+}, Mn^{2+}, Zn^{2+}, and Ni^{2+} (data not shown). Monovalent cations did not affect Ugd_{K-12} activity (data not shown). Chelating the divalent cation with EDTA (Fig. 6) (or EGTA, data not shown) restored the NTP-dependent activation of Ugd_{K-12}.

Mutagenesis of a Putative Allosteric Binding Site on Ugd_{K-12}—The structure of Ugd from *K. pneumoniae* NTUH-K2044 (Ugd_{Kp}) has been determined (11). Ugd_{Kp} shares 83% sequence identity and 93% sequence similarity with Ugd_{K-12} and only differs from Ugd_{K30} by three amino acids. The Ugd_{Kp}-UDPGA complex structure (PDB 3PJG) contained an additional molecule of UDPGA bound at a second site, distinct from the catalytic site. This second UDPGA-binding site lies between the C-terminal Rossmann fold domain (UDP-glucose binding) and the helical subdomain linking this domain to the N-terminal NAD-binding Rossmann fold domain (11). In the Ugd_{Kp}-UDPGA structure, the conformations of Cys-253, Lys-256, and

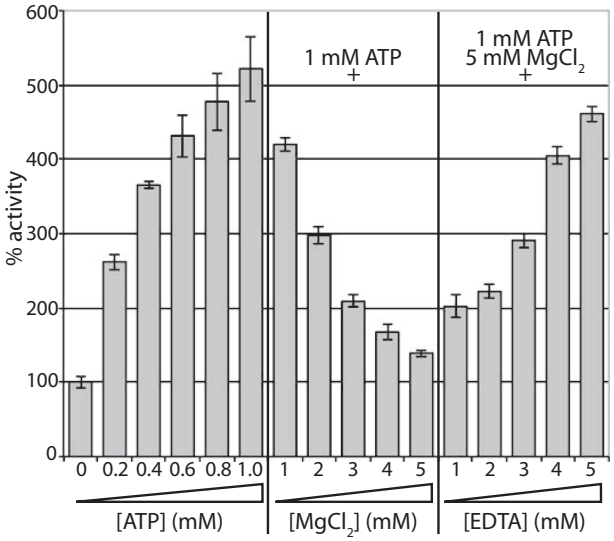

FIGURE 6. **Effect of ATP, Mg^{2+}, and EDTA on Ugd_{K-12} activity.** The activity of Ugd_{K-12} was calculated relative to the no additive control, as in Fig. 2*B*, with increasing ATP, Mg^{2+}, and EDTA. All reactions were performed in triplicate.

Asp-257, all critical for catalysis (60, 61), were shifted out of the catalytic site, and this state of Ugd was therefore proposed to represent the structural state of the enzyme under conditions of known product inhibition (11). Because UDPGA, NAD, and the various nucleotide triphosphates share a common nucleotide structure, it is reasonable to hypothesize that all of these molecules share a single allosteric binding site. This site is defined by the presence of a cluster of basic residues, including Lys-323 and Arg-324 of Ugd_{Kp} (Fig. 1*C*), which hydrogen bonds to the pyrophosphate linkage of UDPGA. Each of these critical basic residues was replaced (individually and together) with alanine. The R324A single and KR → AA double mutants of Ugd_{K-12} purified in much lower amounts relative to wild type; they were prone to degradation and had negligible activity (data not shown). However, the K323A mutant purified similar to wild-type Ugd_{K-12}, with respect to both yield and stability (data not shown). NAD kinetics for the K323A mutant were similar to wild-type Ugd_{K-12} (Table 2), albeit with a slightly lower k_{cat}. When NAD and UDPG were kept constant and ATP was varied, a velocity *versus* ATP concentration plot generated curves that fit Michaelis-Menten kinetics for both the wild-type and K323A mutant proteins (data not shown). The maximal velocities were similar (k_{cat} = 4.6 ± 0.1 and 3.3 ± 0.2 μmol of NADH/min/mg for wild-type and K323A mutant proteins, respectively) but the ATP concentration at one-half the maximum velocity was about 6-fold higher for the K323A mutant ($K_{½}$ = 0.14 ± 0.01 and 0.83 ± 0.16 mM ATP, wild-type and mutant proteins, respectively). The higher $K_{½}$ value caused by the K323A mutation could therefore be explained by a lower binding affinity for ATP compared with Ugd_{K-12}.

DISCUSSION

Ugd synthesizes a critical precursor for the biosynthesis of many bacterial glycans. Although the Ugd homologs from two strains of *E. coli* share a high degree of sequence conservation, they show different kinetic properties; substrate inhibition due to NAD was only a significant factor for Ugd_{K-12}. The kinetics of Ugd_{K30} could be modeled to include NAD substrate inhibition (Fig. 3 and Table 2), but the inhibitory effect was very limited for this homolog and is unlikely to have a profound effect on its *in vivo* activity. The measured cellular concentration of NAD in *E. coli* is in the range of 0.8–1.5 mM depending on the growth phase (43), which is at or slightly below the K_{si} NAD for Ugd_{K-12} (1.4 ± 0.2 mM). The inhibitory effect of NAD at these cellular concentrations will likely impinge on Ugd_{K-12} activity.

In previous studies, purified, nonphosphorylated Ugd_{K-12} was found to have relatively low basal activity (20, 29), but the reaction buffers for those experiments included 5 mM NAD. Based on the kinetic data presented here, the low basal activity could be explained by the substrate inhibition due to the high levels of NAD in the reaction mixtures. Lacour *et al.* (29) also found that Ugd_{K-12} Y71F was folded properly but was almost completely inactive. In this study, inclusion of glycerol in the reaction buffers was essential to stabilize the Y71F mutant and maintain activity. Under these conditions, the mutant and wild-type enzymes possess comparable kinetic properties (Table 2), including NTP-dependent activation

The mechanism of NAD substrate inhibition is not known for Ugd_{K-12}. There are several models available to explain substrate inhibition (44), but one attractive model for Ugd_{K-12} invokes the possibility that multiple molecules of NAD enter the active site. The structure of Ugd_{Kp} (which shares 93% sequence similarity with Ugd_{K-12}) has been solved from a co-crystal of the enzyme with NAD, revealing that the binding pocket for NAD is relatively open (11). At high concentrations of NAD, multiple molecules of the cofactor may fit into the site in nonproductive geometries, giving rise to the observed decrease in dehydrogenase activity. Ugd_{K30} shares a higher degree of conservation with Ugd_{Kp} (differing by only three amino acids), consistent with the proposal that the capsule biosynthesis/export genes lie in a region that may have been horizontally transferred between *E. coli* and *K. pneumoniae* (24). Ugd_{K30} is much less susceptible to NAD substrate inhibition, so the open binding site as observed in Ugd_{Kp} is not sufficient by itself to cause substrate inhibition. Additional structural differences in the Ugd_{K-12} NAD binding pocket may account for the observed differences in substrate inhibition. However, binding of NAD to an allosteric site that negatively impacts the catalytic site is another possible mechanism to explain the substrate inhibition of Ugd_{K-12}.

Allosteric regulation of Ugd is a well established phenomenon. In particular, Ugd_{Kp} shows product inhibition by UDPGA, where UDGPA binds a second pocket adjacent to the catalytic site, and reorganizes several key catalytic residues (11). The compromised binding of ATP (and, to a lesser extent, NAD) in the UDPGA allosteric site of the K323A mutant argues that all three effectors share a common, or overlapping, binding site(s). In particular, it is interesting to note that the uracil-binding portion of this pocket interacts with the nucleotide via Phe-345 and the aliphatic portion of Lys-323, but the pocket does not form hydrogen bonds directly to the nucleotide and is sufficiently open that pyrimidines or purines should be accommodated. This suggests a model where diverse nucleotides can

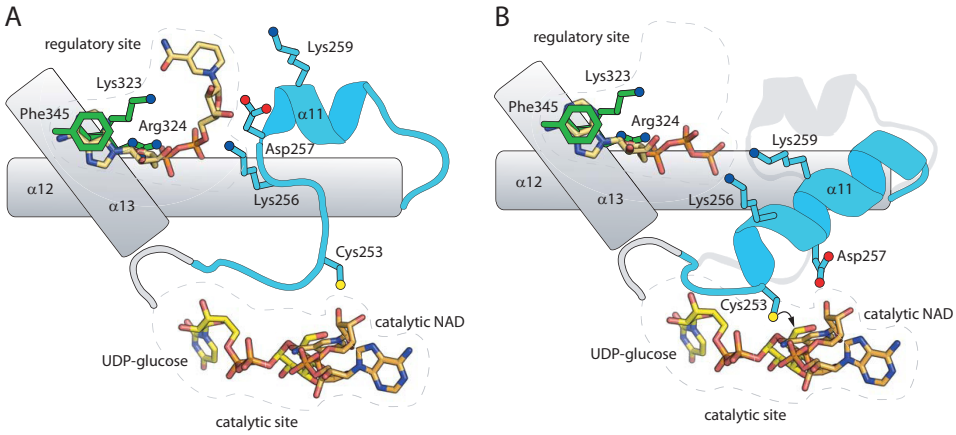

FIGURE 7. **Conceptual model for Ugd regulation.** *A*, in the presence of high concentrations of UDPGA or NAD (shown), these molecules can bind in the regulatory site. Through interactions with residues such as Lys-256 and Asp-257, the mobile loop, including α11, is stabilized in a conformation where Cys-253 is misplaced from the catalytic site, resulting in a conformation that is not competent for turnover (this conformation is seen in UDPGA-bound Ugd_{Kp}, PDB 3PJG (11)). *B*, if a nucleotide triphosphate is bound in this site (ATP depicted), then interactions mediated by the γ-phosphate with residues on α11 (most likely Lys-256 and Lys-259) stabilize this region as a long α-helix in an alternative conformation. This conformation is seen in NAD plus UDP-bound Ugd_{Kp} (PDB 3PLR (11)), except that ATP was modeled in analogy to the second UDPGA in 3PJG. In this conformation, Cys-253 is correctly positioned for attacking the aldehyde moiety of UDPG, and catalysis can proceed. Note that this conformation is likely also stable in the absence of NTP binding, as catalysis is not dependent upon the presence of NTPs under low NAD concentrations.

bind at this site, with one of two potential effects. Binding UDPGA or NAD results in the preferential stabilization of the catalytic loop in a conformation incompatible with efficient turnover (Fig. 7). Alternatively, binding of ATP or related trinucleotides may fail to stabilize the unproductive conformation of this loop, while still competing with NAD and UDPGA for the same binding site. Interactions formed by Asp-257 and Lys-259 with the sugar hydroxyls of UDPGA (and possibly also the ribose of NAD) may be critical determinants in whether the unproductive conformation of the catalytic loop is stabilized. Differences in susceptibility to inhibition may reflect the relative stability of the catalytic loop in its two possible conformations.

Kinetic analysis of $Ugd_{K\text{-}12}$ demonstrated that the NTP-dependent activation and NAD substrate inhibition were linked, *i.e.* the addition of NTP offset the effect of substrate inhibition in a concentration-dependent manner (Fig. 5 and Table 2). The NTP-dependent activation was not nucleotide base-specific as both UTP and ATP could activate $Ugd_{K\text{-}12}$. The lack of activation with NDP addition indicated that the triphosphate moiety was important. However, because pyrophosphate was shown to act as a moderate activator, it is conceivable that only the terminal diphosphate (β- and γ-phosphates of the NTP) is required. An alternative model is that the third phosphate is required to compensate for unfavorable interactions mediated by the nucleotide. Divalent cations greatly reduce the effectiveness of ATP in relieving inhibition, probably because the NTP-cation complex lacks sufficient electronegativity to bind favorably in the highly electropositive binding pocket.

The concentration of ATP required to remove substrate inhibition is lower than the reported intracellular concentration of 3 mM for *E. coli* (45), so it is likely that any substrate inhibition of $Ugd_{K\text{-}12}$ would be diminished *in vivo*, especially considering that the source of stimulation is not confined to ATP (Fig. 2*B*). However, confidently assessing the contributions is difficult because the competing effects are further complicated by the concentration of free Mg^{2+} in *E. coli* (reported to be between 1 and 2 mM (46)), which would at least partly attenuate the NTP-dependent stimulatory effect. Any local variation in the concentrations of ATP and Mg^{2+} (and NAD) in the microenvironments of $Ugd_{K\text{-}12}$ could also exert an effect. In essence, small alterations in the local concentrations for any of these molecules could enable the modulation of Ugd activity affecting the production of UDPGA and subsequent downstream products (*e.g.* extracellular polysaccharide).

The data reported here indicate that, in contrast to previous publications (20, 29), phosphorylation of Tyr-71 is not required for Ugd activity. The structure of Ugd_{Kp} (which shares high sequence identity with $Ugd_{K\text{-}12}$) positions Tyr-71 relatively deep within the NAD-binding site (Fig. 1*C*) (11). There is some evidence that BY-kinases bind their substrates as extended peptides. In the crystal of the tyrosine kinase domain of the *Staphylococcus aureus* Wzc homolog, CapB, the tyrosine-rich C terminus of one monomer adopted an extended conformation to bind in the active site of an adjacent monomer (47). Therefore, phosphorylation of Tyr-71 in Ugd would require local unfolding to place the tyrosine in the catalytic site of the kinase. In contrast, phosphorylation of UDP-*N*-acetylmannosamine dehydrogenase (Cap5O) by the Cap5B BY-kinase from *S. aureus* occurs at a tyrosine residue that is surface-exposed in the solved structure (48). The activity of the modified enzyme is increased 2–3-fold above the basal (unmodified) level. The Ugd homolog from *B. subtilis* (Ugd_{Bs}) could be phosphorylated *in vitro* leading to an increase (2-fold) in dehydrogenase activity (19). Although no structure is available for Ugd_{Bs}, a structural model generated by structure-based sequence alignment located the proposed tyrosine residue on the surface of the protein (49), potentially making it accessible to kinase. Consistent with this, phosphorylated Ugd_{Bs} was identified in a phosphoproteomics study (50), although it was not clear if it was the tyrosine or an adjacent serine that was phosphorylated. $Ugd_{K\text{-}12}$ was not identified in a similar phosphoproteomics study in *E. coli,* but it is unclear whether the BY-kinases were active under the conditions used (51); notably, neither of the auto-

phosphorylating BY-kinases (Etk and Wzc) (25, 52) were detected in the phosphoproteome under the same conditions. The absence of any effect of Tyr-71 mutations could be explained by phosphorylation at a different site. For example, TuaD (another Ugd homolog in *B. subtilis* involved in teichuronic acid production) was activated upon phosphorylation but does not have a tyrosine residue in the position equivalent to the Tyr-71 of Ugd_{Bs} (19). However, we were unable to identify conditions that gave convincing phosphorylation of Ugd_{K30} or Ugd_{K-12} in the *E. coli* K30 background, despite clear activity for Wzc_{K30} (data not shown). Also, induction of colanic acid production in wild-type *E. coli* K-12 strain, W3110, caused increased *wzc* expression, but no concomitant phosphorylation of Ugd was detected (data not shown). Low level, nonspecific phosphorylation of Cap5O was reported and interpreted as a reflection of the flexibility of the Cap5B kinase (48). Whether this extends to Wzc/Etk is unclear. The regulation of extracellular polysaccharide production is a complex process. The data reported here indicate that different homologs of Ugd exhibit altered properties in two isolates of *E. coli* despite a highly conserved sequence. The regulation of *ugd* in *E. coli* K-12 is a multilayered process. In some bacteria, the *ugd* gene itself is regulated by as many as three different phosphorelay systems. In *E. coli*, ugd_{K-12} was found to be within the top 10 genes that were up-regulated by the RcsC/YojN/RcsB/RcsA phosphorelay system as part of the Rcs regulon (53); the regulon includes a wide range of genes associated with cell envelope assembly and homeostasis, including colanic acid production (22). Ugd_{K-12} regulation is also impacted by both PmrA/PmrB and PhoP/PhoQ, and this may influence the need for RcsA (54). The data presented here demonstrate that unique features of the enzyme kinetics of Ugd_{K-12} also provide an additional level of post-translational control, potentially allowing instantaneous response to particular environmental cues. In contrast, group 1 CPSs are constitutively expressed in *E. coli* and *K. pneumoniae*, where they are important virulence factors. The *cps* locus is not responsive to RcsC/YojN/RcsB/(RcsA) (23) in *E. coli* with group 1 CPSs. Enhanced CPS production in these strains results from Rcs-mediated up-regulation of the *galF* gene, whose product is implicated in the biosynthesis of a UDP-glucose precursor (55). The sequences upstream of ugd_{K-12} and ugd_{K30} differ, with the latter lacking an evident PmrA box (data not shown) suggesting different regulation. In these bacteria, Ugd_{K30} is active under conditions where Rcs-mediated up-regulation is not anticipated, and it lacks the subtle modulation of activity seen in Ugd_{K-12}. Why two Ugd homologs from different *E. coli* strains would differ in post-translational regulatory properties remains unclear.

Acknowledgments—We thank Jason Carere and Scott Mazurkewich for technical advice regarding enzyme kinetics.

REFERENCES

1. Clarkin, C. E., Allen, S., Kuiper, N. J., Wheeler, B. T., Wheeler-Jones, C. P., and Pitsillides, A. A. (2011) Regulation of UDP-glucose dehydrogenase is sufficient to modulate hyaluronan production and release, control sulfated GAG synthesis, and promote chondrogenesis. *J. Cell Physiol.* **226,** 749–761
2. Alvarez, D., Merino, S., Tomás, J. M., Benedí, V. J., and Albertí, S. (2000) Capsular polysaccharide is a major complement resistance factor in lipopolysaccharide O side chain-deficient *Klebsiella pneumoniae* clinical isolates. *Infect. Immun.* **68,** 953–955
3. Wessels, M. R., Goldberg, J. B., Moses, A. E., and DiCesare, T. J. (1994) Effects on virulence of mutations in a locus essential for hyaluronic acid capsule expression in group A streptococci. *Infect. Immun.* **62,** 433–441
4. Raetz, C. R., Reynolds, C. M., Trent, M. S., and Bishop, R. E. (2007) Lipid A modification systems in Gram-negative bacteria. *Annu. Rev. Biochem.* **76,** 295–329
5. Strominger, J. L., Kalckar, H. M., Axelrod, J., and Maxwell, E. S. (1954) Enzymatic oxidation of uridine diphosphate glucose to uridine diphosphate glucuronic acid. *J. Am. Chem. Soc.* **76,** 6411–6412
6. Egger, S., Chaikuad, A., Kavanagh, K. L., Oppermann, U., and Nidetzky, B. (2010) UDP-glucose dehydrogenase: structure and function of a potential drug target. *Biochem. Soc. Trans.* **38,** 1378–1385
7. Egger, S., Chaikuad, A., Kavanagh, K. L., Oppermann, U., and Nidetzky, B. (2011) Structure and mechanism of human UDP-glucose 6-dehydrogenase. *J. Biol. Chem.* **286,** 23877–23887
8. Kadirvelraj, R., Sennett, N. C., Polizzi, S. J., Weitzel, S., and Wood, Z. A. (2011) Role of packing defects in the evolution of allostery and induced fit in human UDP-glucose dehydrogenase. *Biochemistry* **50,** 5780–5789
9. Hung, R. J., Chien, H. S., Lin, R. Z., Lin, C. T., Vatsyayan, J., Peng, H. L., and Chang, H. Y. (2007) Comparative analysis of two UDP-glucose dehydrogenases in *Pseudomonas aeruginosa* PAO1. *J. Biol. Chem.* **282,** 17738–17748
10. Schiller, J. G., Bowser, A. M., and Feingold, D. S. (1973) Partial purification and properties of UDPG dehydrogenase from *Escherichia coli*. *Biochim. Biophys. Acta* **293,** 1–10
11. Chen, Y. Y., Ko, T. P., Lin, C. H., Chen, W. H., and Wang, A. H. (2011) Conformational change upon product binding to *Klebsiella pneumoniae* UDP-glucose dehydrogenase: a possible inhibition mechanism for the key enzyme in polymyxin resistance. *J. Struct. Biol.* **175,** 300–310
12. Grangeasse, C., Cozzone, A. J., Deutscher, J., and Mijakovic, I. (2007) Tyrosine phosphorylation: an emerging regulatory device of bacterial physiology. *Trends Biochem. Sci.* **32,** 86–94
13. Cuthbertson, L., Mainprize, I. L., Naismith, J. H., and Whitfield, C. (2009) Pivotal roles of the outer membrane polysaccharide export and polysaccharide copolymerase protein families in export of extracellular polysaccharides in Gram-negative bacteria. *Microbiol. Mol. Biol. Rev.* **73,** 155–177
14. Shi, L., Kobir, A., Jers, C., and Mijakovic, I. (2010) Bacterial protein-tyrosine kinases. *Curr. Proteomics* **7,** 188–194
15. Drummelsmith, J., and Whitfield, C. (1999) Gene products required for surface expression of the capsular form of the group 1 K antigen in *Escherichia coli* (O9a: K30). *Mol. Microbiol.* **31,** 1321–1332
16. Stevenson, G., Andrianopoulos, K., Hobbs, M., and Reeves, P. R. (1996) Organization of the *Escherichia coli* K-12 gene cluster responsible for production of the extracellular polysaccharide colanic acid. *J. Bacteriol.* **178,** 4885–4893
17. Collins, R. F., Beis, K., Dong, C., Botting, C. H., McDonnell, C., Ford, R. C., Clarke, B. R., Whitfield, C., and Naismith, J. H. (2007) The 3D structure of a periplasm-spanning platform required for assembly of group 1 capsular polysaccharides in *Escherichia coli*. *Proc. Natl. Acad. Sci. U.S.A.* **104,** 2390–2395
18. Dong, C., Beis, K., Nesper, J., Brunkan-Lamontagne, A. L., Clarke, B. R., Whitfield, C., and Naismith, J. H. (2006) Wza the translocon for *E. coli* capsular polysaccharides defines a new class of membrane protein. *Nature* **444,** 226–229
19. Mijakovic, I., Poncet, S., Boël, G., Mazé, A., Gillet, S., Jamet, E., Decottignies, P., Grangeasse, C., Doublet, P., Le Maréchal, P., and Deutscher, J. (2003) Transmembrane modulator-dependent bacterial tyrosine kinase activates UDP-glucose dehydrogenases. *EMBO J.* **22,** 4709–4718
20. Grangeasse, C., Obadia, B., Mijakovic, I., Deutscher, J., Cozzone, A. J., and Doublet, P. (2003) Autophosphorylation of the *Escherichia coli* protein kinase Wzc regulates tyrosine phosphorylation of Ugd, a UDP-glucose dehydrogenase. *J. Biol. Chem.* **278,** 39323–39329

21. Whitfield, C. (2006) Biosynthesis and assembly of capsular polysaccharides in *Escherichia coli*. *Annu. Rev. Biochem.* **75,** 39–68
22. Majdalani, N., and Gottesman, S. (2005) The Rcs phosphorelay: a complex signal transduction system. *Annu. Rev. Microbiol.* **59,** 379–405
23. Rahn, A., and Whitfield, C. (2003) Transcriptional organization and regulation of the *Escherichia coli* K30 group 1 capsule biosynthesis (*cps*) gene cluster. *Mol. Microbiol.* **47,** 1045–1060
24. Rahn, A., Drummelsmith, J., and Whitfield, C. (1999) Conserved organization in the *cps* gene clusters for expression of *Escherichia coli* group 1 K antigens: relationship to the colanic acid biosynthesis locus and the *cps* genes from *Klebsiella pneumoniae*. *J. Bacteriol.* **181,** 2307–2313
25. Ilan, O., Bloch, Y., Frankel, G., Ullrich, H., Geider, K., and Rosenshine, I. (1999) Protein tyrosine kinases in bacterial pathogens are associated with virulence and production of exopolysaccharide. *EMBO J.* **18,** 3241–3248
26. Wugeditsch, T., Paiment, A., Hocking, J., Drummelsmith, J., Forrester, C., and Whitfield, C. (2001) Phosphorylation of Wzc, a tyrosine autokinase, is essential for assembly of group 1 capsular polysaccharides in *Escherichia coli*. *J. Biol. Chem.* **276,** 2361–2371
27. Bechet, E., Gruszczyk, J., Terreux, R., Gueguen-Chaignon, V., Vigouroux, A., Obadia, B., Cozzone, A. J., Nessler, S., and Grangeasse, C. (2010) Identification of structural and molecular determinants of the tyrosine kinase Wzc and implications in capsular polysaccharide export. *Mol. Microbiol.* **77,** 1315–1325
28. Lee, D. C., Zheng, J., She, Y. M., and Jia, Z. (2008) Structure of *Escherichia coli* tyrosine kinase Etk reveals a novel activation mechanism. *EMBO J.* **27,** 1758–1766
29. Lacour, S., Bechet, E., Cozzone, A. J., Mijakovic, I., and Grangeasse, C. (2008) Tyrosine phosphorylation of the UDP-glucose dehydrogenase of *Escherichia coli* is at the crossroads of colanic acid synthesis and polymyxin resistance. *PLoS One* **3,** e3053
30. Bertani, G. (1951) Studies on lysogenesis. I. The mode of phage liberation by lysogenic *Escherichia coli*. *J. Bacteriol.* **62,** 293–300
31. Datsenko, K. A., and Wanner, B. L. (2000) One-step inactivation of chromosomal genes in *Escherichia coli* K-12 using PCR products. *Proc. Natl. Acad. Sci. U.S.A.* **97,** 6640–6645
32. Cherepanov, P. P., and Wackernagel, W. (1995) Gene disruption in *Escherichia coli*: TcR and KmR cassettes with the option of Flp-catalyzed excision of the antibiotic resistance determinant. *Gene* **158,** 9–14
33. Xayarath, B., and Yother, J. (2007) Mutations blocking side chain assembly, polymerization, or transport of a Wzy-dependent *Streptococcus pneumoniae* capsule are lethal in the absence of suppressor mutations and can affect polymer transfer to the cell wall. *J. Bacteriol.* **189,** 3369–3381
34. Yuasa, R., Levinthal, M., and Nikaido, H. (1969) Biosynthesis of cell wall lipopolysaccharide in mutants of *Salmonella*. V. A mutant of *Salmonella typhimurium* defective in the synthesis of cytidine diphosphoabequose. *J. Bacteriol.* **100,** 433–444
35. Whitfield, C., and Paiment, A. (2003) Biosynthesis and assembly of group 1 capsular polysaccharides in *Escherichia coli* and related extracellular polysaccharides in other bacteria. *Carbohydr. Res.* **338,** 2491–2502
36. Boels, I. C., Ramos, A., Kleerebezem, M., and de Vos, W. M. (2001) Functional analysis of the *Lactococcus lactis galU* and *galE* genes and their impact on sugar nucleotide and exopolysaccharide biosynthesis. *Appl. Environ. Microbiol.* **67,** 3033–3040
37. Jayaratne, P., Bronner, D., MacLachlan, P. R., Dodgson, C., Kido, N., and Whitfield, C. (1994) Cloning and analysis of duplicated *rfbM* and *rfbK* genes involved in the formation of GDP-mannose in *Escherichia coli* O9:K30 and participation of *rfb* genes in the synthesis of the group I K30 capsular polysaccharide. *J. Bacteriol.* **176,** 3126–3139
38. Pagni, M., Lazarevic, V., Soldo, B., and Karamata, D. (1999) Assay for UDPglucose-6-dehydrogenase in phosphate-starved cells: gene *tuaD* of *Bacillus subtilis* 168 encodes the UDP-glucose-6-dehydrogenase involved in teichuronic acid synthesis. *Microbiology* **145,** 1049–1053
39. Hitchcock, P. J., and Brown, T. M. (1983) Morphological heterogeneity among *Salmonella* lipopolysaccharide chemotypes in silver-stained polyacrylamide gels. *J. Bacteriol.* **154,** 269–277
40. Dodgson, C., Amor, P., and Whitfield, C. (1996) Distribution of the *rol* gene encoding the regulator of lipopolysaccharide O-chain length in *Escherichia coli* and its influence on the expression of group I capsular K antigens. *J. Bacteriol.* **178,** 1895–1902
41. Reid, A. N., and Whitfield, C. (2005) Functional analysis of conserved gene products involved in assembly of *Escherichia coli* capsules and exopolysaccharides: evidence for molecular recognition between Wza and Wzc for colanic acid biosynthesis. *J. Bacteriol.* **187,** 5470–5481
42. Campbell, R. E., Sala, R. F., van de Rijn, I., and Tanner, M. E. (1997) Properties and kinetic analysis of UDP-glucose dehydrogenase from group A streptococci. Irreversible inhibition by UDP-chloroacetol. *J. Biol. Chem.* **272,** 3416–3422
43. Dhamdhere, G., and Zgurskaya, H. I. (2010) Metabolic shutdown in *Escherichia coli* cells lacking the outer membrane channel TolC. *Mol. Microbiol.* **77,** 743–754
44. Reed, M. C., Lieb, A., and Nijhout, H. F. (2010) The biological significance of substrate inhibition: a mechanism with diverse functions. *BioEssays* **32,** 422–429
45. Buckstein, M. H., He, J., and Rubin, H. (2008) Characterization of nucleotide pools as a function of physiological state in *Escherichia coli*. *J. Bacteriol.* **190,** 718–726
46. Alatossava, T., Jütte, H., Kuhn, A., and Kellenberger, E. (1985) Manipulation of intracellular magnesium content in polymyxin B nonapeptide-sensitized *Escherichia coli* by ionophore A23187. *J. Bacteriol.* **162,** 413–419
47. Olivares-Illana, V., Meyer, P., Bechet, E., Gueguen-Chaignon, V., Soulat, D., Lazereg-Riquier, S., Mijakovic, I., Deutscher, J., Cozzone, A. J., Laprévote, O., Morera, S., Grangeasse, C., and Nessler, S. (2008) Structural basis for the regulation mechanism of the tyrosine kinase CapB from *Staphylococcus aureus*. *PLoS Biol.* **6,** e143
48. Gruszczyk, J., Fleurie, A., Olivares-Illana, V., Béchet, E., Zanella-Cleon, I., Moréra, S., Meyer, P., Pompidor, G., Kahn, R., Grangeasse, C., and Nessler, S. (2011) Structure analysis of the *Staphylococcus aureus* UDP-*N*-acetylmannosamine dehydrogenase Cap5O involved in capsular polysaccharide biosynthesis. *J. Biol. Chem.* **286,** 17112–17121
49. Petranovic, D., Grangeasse, C., Macek, B., Abdillatef, M., Gueguen-Chaignon, V., Nessler, S., Deutscher, J., and Mijakovic, I. (2009) Activation of *Bacillus subtilis* Ugd by the BY-kinase PtkA proceeds via phosphorylation of its residue tyrosine 70. *J. Mol. Microbiol. Biotechnol.* **17,** 83–89
50. Macek, B., Mijakovic, I., Olsen, J. V., Gnad, F., Kumar, C., Jensen, P. R., and Mann, M. (2007) The serine/threonine/tyrosine phosphoproteome of the model bacterium *Bacillus subtilis*. *Mol. Cell. Proteomics* **6,** 697–707
51. Macek, B., Gnad, F., Soufi, B., Kumar, C., Olsen, J. V., Mijakovic, I., and Mann, M. (2008) Phosphoproteome analysis of *E. coli* reveals evolutionary conservation of bacterial Ser/Thr/Tyr phosphorylation. *Mol. Cell. Proteomics* **7,** 299–307
52. Vincent, C., Doublet, P., Grangeasse, C., Vaganay, E., Cozzone, A. J., and Duclos, B. (1999) Cells of *Escherichia coli* contain a protein-tyrosine kinase, Wzc, and a phosphotyrosine-protein phosphatase, Wzb. *J. Bacteriol.* **181,** 3472–3477
53. Ferrières, L., and Clarke, D. J. (2003) The RcsC sensor kinase is required for normal biofilm formation in *Escherichia coli* K-12 and controls the expression of a regulon in response to growth on a solid surface. *Mol. Microbiol.* **50,** 1665–1682
54. Mouslim, C., and Groisman, E. A. (2003) Control of the *Salmonella ugd* gene by three two-component regulatory systems. *Mol. Microbiol.* **47,** 335–344
55. Ho, J. Y., Lin, T. L., Li, C. Y., Lee, A., Cheng, A. N., Chen, M. C., Wu, S. H., Wang, J. T., Li, T. L., and Tsai, M. D. (2011) Functions of some capsular polysaccharide biosynthetic genes in *Klebsiella pneumoniae* NTUH K-2044. *PLoS One* **6,** e21664
56. Guzman, L. M., Belin, D., Carson, M. J., and Beckwith, J. (1995) Tight regulation, modulation, and high-level expression by vectors containing the arabinose PBAD promoter. *J. Bacteriol.* **177,** 4121–4130
57. Keenleyside, W. J., Jayaratne, P., MacLachlan, P. R., and Whitfield, C. (1992) The *rcsA* gene of *Escherichia coli* O9:K30:H12 is involved in the expression of the serotype-specific group I K (capsular) antigen. *J. Bacteriol.* **174,** 8–16
58. Drummelsmith, J., Amor, P. A., and Whitfield, C. (1997) Polymorphism, duplication, and IS1-mediated rearrangement in the chromosomal *his-*

rfb-gnd region of *Escherichia coli* strains with group IA and capsular K antigens. *J. Bacteriol.* **179,** 3232–3238
59. Chenna, R., Sugawara, H., Koike, T., Lopez, R., Gibson, T. J., Higgins, D. G., and Thompson, J. D. (2003) Multiple sequence alignment with the Clustal series of programs. *Nucleic Acids Res.* **31,** 3497–3500
60. Sommer, B. J, Barycki, J. J., and Simpson, M. A. (2004) Characterization of human UDP-glucose dehydrogenase. CYS-276 is required for the second of two successive oxidations. *J. Biol. Chem.* **279,** 23590–23596
61. Easley, K. E., Sommer, B. J., Boanca, G., Barycki, J. J., and Simpson, M. A. (2007) Characterization of human UDP-glucose dehydrogenase reveals critical catalytic roles for lysine 220 and aspartate 280. *Biochemistry* **46,** 369–378